

Isotope shift, non-linearity of King plot and search for nuclear island of stability and new particles

V. V. Flambaum^{1,2}, A. J. Geddes¹, and A. V. Viatkina²

¹*School of Physics, University of New South Wales, Sydney 2052, Australia and*

²*Helmholtz Institute Mainz, Johannes Gutenberg University, 55099 Mainz, Germany*

(Dated: December 14, 2024)

The Racah-Rosenthal-Breit formula describes the isotope field shift for s-wave only and is not valid in heavy atoms where the relativistic effects are important. We derive a single-particle relativistic formula for the isotope shift for an arbitrary electron angular momentum; we then apply it to estimate the differences in the transition frequencies between the superheavy atoms produced in laboratory and atoms with nuclei belonging to the hypothetical island of stability (these nuclei have a "magical" number of neutrons $N = 184$). Our results may be applied to the search for metastable neutron-rich isotopes in astrophysical atomic spectra using the known values of the transition frequencies for the neutron deficient isotopes produced in laboratory. An example may be the spectra of the Przybylski's star where superheavy elements up to $Z = 99$ have been possibly identified. We have found that the nuclear polarizability contribution leads to the significant deviation of the King plot for isotope shifts from the linearity. Therefore, the measurements of the non-linearity of King plots may be applied to measure the nuclear polarizability change between individual isotopes. It was recently suggested that such measurements may also be used to search for new particles mediating Yukawa-type interactions in atoms. We estimate the non-linear corrections to the King plot including contributions of the relativistic effects in the field shift, isotope shift due to the nuclear polarizability, many-body effects and effect of hypothetical new particles. Our estimates provide theoretical limitations on the sensitivity of such a search and should help in selection of the most suitable atoms for corresponding experiments.

I. INTRODUCTION

The isotope shift (IS) phenomena in heavy atoms is an important way of probing various scenarios in nuclear physics and can aid the search for new physics beyond the Standard Model.

Nuclear theory predicts the existence of long-lived isotopes for elements with $Z \geq 104$ (see e.g. [1, 2]), in particular isotopes with a magic neutron number $N = 184$. However, producing these neutron-rich isotopes in laboratories by colliding lighter atoms is currently impossible. The Coulomb repulsion for nuclei grows as Z^2 ; in order to compensate for this with the attractive strong force, the neutron number N must grow faster than Z . Consequently, an isotope from the island of stability with $N = 184$ cannot be produced from the collision of a pair of lighter isotopes with smaller N/Z ratios.

In contrast to laboratories, astrophysical events such as supernovae explosions, neutron stars and neutron star - black hole mergers that produce a high neutron flux create environments that may be favorable to the production of neutron-rich heavy elements. A new mechanism due to the capture of the neutron star material by a primordial black hole has been suggested in [3]. It may be possible to thus predict the spectral lines of a neutron-rich, metastable isotope based on the experimental spectrum of a neutron-poor isotope of a given element and an accurate numerical calculation of IS. The results can then be used to search for the long-lifetime neutron-rich elements in astrophysical spectra, e.g. in the spectra of Przybylski's star. It is possible that optical lines of elements up to $Z = 99$ have already been identified in

the aforementioned spectra [4]. These elements include heavy, short-lived isotopes which may be products of the decay of long-lifetime nuclei near the island of stability [5]. Therefore, determining the IS for superheavy elements can help trace the hypothetical island of stability in astrophysical data.

Spectroscopic measurements of IS may be also relevant to the search for strange matter. Regular nuclei consisting of protons and neutrons can be, in fact, metastable states which decay into nuclei consisting of up, down and strange quarks (see [6] and references therein) or the strange matter nuclei may be metastable. The strange matter nuclei of charge Z would have a very different radius comparing to any regular isotope. A reliable formula for IS can be used to predict the effects of this change in radius on atomic spectra.

Accurate numerical calculations of IS for heavy and superheavy elements are usually produced using sophisticated many-body theory methods, for example, combining a configuration interaction (CI) and many-body perturbation theory approach (MBPT) (see e.g. [5] and the references there). However, in the absence of experimental data a simple analytical formula may be useful for quick estimates of IS and better qualitative understanding of this phenomenon. Accordingly, we derive a relativistic mean-field analytic formula for the field shift, which is the dominating source of the IS in heavy atoms.

The relativistic corrections produce an important difference in the dependence of the field shift on the nuclear radius r . The field shift becomes different from the traditional expression $F_i \delta \langle r^2 \rangle$. Instead, one has $\tilde{F}_i \delta \langle r^{2\gamma} \rangle$, where $\gamma = [(j + 1/2)^2 - Z^2 \alpha^2]^{1/2}$, j is the electron an-

gular momentum, F_i and \tilde{F}_i are the electronic structure factors; \tilde{F}_i is calculated in the present work. If one insists on using the traditional formula for the field shift $F_i \delta \langle r^2 \rangle$, the factor F_i will depend on the nuclear radius, i.e. there will be no factorisation of the electron and nuclear variables.

Due to the relativistic effects in heavy atoms the field shift of $p_{1/2}$ orbital is comparable to the $s_{1/2}$ one: the ratio is $\sim (1-\gamma)/(1+\gamma)$. The $Z\alpha$ expansion gives the ratio $\sim Z^2\alpha^2/4$ but for $Z=137$ $\gamma \approx 0$ and for the superheavy elements the ratio tends to 1. For higher waves the direct single-particle field shift is small. However, the core relaxation effect (the correction to the atomic potential δV due to the perturbation of the s and $p_{1/2}$ orbitals by the field shift operator) makes the field shift for all orbitals have the same dependence on the nuclear radius: $\tilde{F}_i \delta \langle r^{2\gamma} \rangle$, where $\gamma = [1 - Z^2\alpha^2]^{1/2}$.

In addition, since the relative magnitude of the many-body corrections to the mean-field case is approximately the same for atoms with similar electron structure of outer shells, our formula may be used to make reasonable extrapolations from the experimental data of lighter atoms to superheavy elements where no data are available.

Our formulas for the field IS also allow us to estimate a King plot nonlinearity of a given element. New long-range forces such as Yukawa-type interactions between electrons and nucleus can lead to nonlinearities in a King plot in a series of isotopes [7]. It is necessary to understand all other sources of nonlinearities in the IS in order to search for possible new physics beyond the Standard Model. We estimate the core relaxation corrections and quadratic effects in the field shift. We also estimate the contribution to IS from the nuclear polarizability which actually gives a bigger contribution to the King plot nonlinearity than the relativistic corrections to the field shift. This fact allows an experimental probe of the change of nuclear polarizability between isotopes based on measuring the King plot non-linearity.

II. FIELD SHIFT IN THE MEAN FIELD APPROXIMATION

In [8, 9] the Racah-Rosenthal-Breit formula for IS of s -wave energy levels was derived using first-order perturbation theory. However it is found that for relativistic cases the formula is unjustified, as it relies on perturbation theory using the the Coulomb wave functions for a point-like nucleus when finding the correction to the energy due to the finite nuclear size. This is not valid because, while the energy perturbation due to the potential inside the nucleus is small, the perturbed and non-perturbed wave functions within this region are completely different. Indeed, the relativistic wave functions for $s_{1/2}$ and $p_{1/2}$ orbitals tend to infinity at $r = 0$ while for the finite nucleus they remain finite. Numerous attempts were made to account for this large wave function distortion (see [10]

p. 38 and references therein). Furthermore, it should be pointed out that a high-precision analytical formula for the finite nuclear size corrections in one electron atoms and ions was developed, taking into account the fine details of nuclear charge distribution [11]. However, we need the results for many-electron atoms and ions.

In this work, we aim to find a simple analytical expression of the field IS in many-electron atoms for arbitrary valence electron angular momenta j, l based on the first-order perturbation theory, but starting from a more realistic initial approximation than a point-like nucleus. In our final formula, we also avoid using the factor equal to the nonrelativistic probability density of the electron at the point nucleus $|\psi(0)|^2$, which needs further evaluation.

A. Single-particle isotope shift in many-electron atoms for arbitrary orbital angular momentum

The dominant contribution to IS in heavy atoms is the field shift arising from the change of nuclear radius, relative to mass shift which is smaller [12]. Let us first consider a model allowing for the estimation of field IS for wave functions with arbitrary Dirac quantum number $\kappa = \mp (j + \frac{1}{2})$, where $j = l \pm \frac{1}{2}$. Through this work we assume the nucleus to be a uniformly charged sphere of radius R . The nuclear potential can be written as:

$$V(r, R) = \begin{cases} -\frac{Ze^2}{r} & \text{for } r \geq R \\ -\frac{Ze^2}{R} \left(\frac{3}{2} - \frac{r^2}{2R^2} \right) & \text{for } r \leq R \end{cases} \quad (1)$$

Our perturbation is the change of the potential due to small relative change of nuclear radii between isotopes which can be defined as

$$\delta V = \frac{dV(r, R)}{dR} \delta R = \frac{3Ze^2}{2R} \left(1 - \frac{r^2}{R^2} \right) \frac{\delta R}{R}. \quad (2)$$

Using perturbation theory and integrating over the nucleus we can find the shift in energy as

$$\delta \epsilon_\kappa = \int_{\text{nuc.}} \Psi_\kappa^\dagger \delta V \Psi_\kappa d\vec{r}. \quad (3)$$

Radial parts of wave functions can be found from the following Dirac system of radial equations:

$$\begin{cases} \left(\frac{d}{dr} + \frac{\kappa}{r} \right) r f(r) = (m + E - V) r g(r), \\ \left(\frac{d}{dr} - \frac{\kappa}{r} \right) r g(r) = (m - E + V) r f(r). \end{cases} \quad (4)$$

We approximate the potential energy near $r = 0$ to be constant:

$$u = V(0) = -\frac{3Ze^2}{2R}, \quad E, m \ll u. \quad (5)$$

After equating $F = r f(r)$ and $G = r g(r)$ we find that

$$\begin{cases} F' + \frac{\kappa}{r} F + uG = 0, \\ G' - \frac{\kappa}{r} G - uF = 0. \end{cases} \quad (6)$$

One can check that the solutions at small distances can be written as

$$\begin{aligned} \kappa < 0 : F &= ar^{|\kappa|} + a_1 r^{|\kappa|+2}, \quad G = \frac{au}{2|\kappa|+1} r^{|\kappa|+1}, \\ \kappa > 0 : G &= br^{|\kappa|} + b_1 r^{|\kappa|+2}, \quad F = -\frac{bu}{2|\kappa|+1} r^{|\kappa|+1}. \end{aligned}$$

where a, b are normalization constants and

$$a_1 = -\frac{u^2 a}{2(2|\kappa|+1)}, \quad b_1 = -\frac{u^2 b}{2(2|\kappa|+1)}.$$

Here we neglected higher orders in r^2/R^2 . More accurate calculations have demonstrated that their contribution to the field IS is small (see next subsection).

It can be shown that in both cases

$$(F^2 + G^2) \propto r^{2|\kappa|} \left(1 - \frac{9}{2} \frac{Z^2 \alpha^2 |\kappa|}{(2|\kappa|+1)^2} \left(\frac{r}{R} \right)^2 \right). \quad (7)$$

To determine the field IS we match the expression for the radial density $f^2 + g^2$ inside the nucleus to the radial density outside the nucleus. At the surface $\rho_{inside} = \rho_{outside}$, since ρ is continuous. Near the nucleus the nuclear Coulomb potential is not screened, and all atomic wave functions are proportional to the corresponding Coulomb wave functions. Therefore we use expressions of these wave functions at small distances (presented in the Appendix C) to approximate the density on the nuclear surface ($r = R$):

$$\begin{aligned} \rho_{sf} &= f_{sf}^2 + g_{sf}^2 \\ &= \frac{1}{(z_i+1) a_b^3} \left(\frac{I}{Ry} \right)^{3/2} \frac{4}{[\Gamma(2\gamma+1)]^2} \left(\frac{a_b}{2ZR} \right)^{2-2\gamma} \\ &\quad \times \left[(\kappa - \gamma)^2 + Z^2 \alpha^2 \right] \\ &= \frac{1}{(z_i+1) a_b^3} \left(\frac{I}{Ry} \right)^{3/2} \frac{4}{[\Gamma(2\gamma+1)]^2} \left(\frac{a_b}{2ZR} \right)^{2-2\gamma} \\ &\quad \times 2\kappa(\kappa - \gamma), \end{aligned} \quad (8)$$

where $\gamma = \sqrt{\kappa^2 - Z^2 \alpha^2}$. As has been shown above, density inside the nucleus approximately behaves as:

$$\rho(r) \approx \rho_{sf} \left(\frac{r}{R} \right)^{2(|\kappa|-1)} \quad (9)$$

This expression approximates the electron density inside the nucleus significantly better than the Coulomb solution and should give more accurate results than the the Racah-Rosenthal-Breit approach. Corrections to Eqs. (7, 8, 9) will be discussed in the next section. Their contribution to the isotope shift has been found to be small.

Using Eq. (3) and introducing $x = r/R$ one can find that

$$\begin{aligned} \delta\epsilon_\kappa &= \frac{3}{2} Z e^2 R^2 \frac{\delta R}{R} \int_0^1 (f_\kappa^2 + g_\kappa^2) (1-x^2) x^2 dx \\ &= \frac{3}{2} Z e^2 R^2 \frac{\delta R}{R} \int_0^1 \rho_{sf} x^{2(|\kappa|-1)} (1-x^2) x^2 dx, \end{aligned} \quad (10)$$

which gives

$$\begin{aligned} \delta\epsilon_\kappa &= \frac{1}{(z_i+1) (2|\kappa|+1) (2|\kappa|+3) [\Gamma(2\gamma+1)]^2} \\ &\quad \times \left(\frac{2ZR}{a_b} \right)^{2\gamma} \frac{I^{3/2}}{Ry^{1/2}} \frac{\delta R}{R}. \end{aligned} \quad (11)$$

Here $I \equiv |\epsilon_\kappa| = \frac{(z_i+1)^2}{\nu^2} Ry$ is the ionization energy for an orbital with effective principal quantum number ν in the ion of charge z_i , and $Ry = \frac{e^2}{2a_b}$ is the Rydberg constant.

B. Isotope shift for s and $p_{1/2}$ waves

From Eq. (7) we see that $Z^2 \alpha^2 r^2/R^2$ corrections to the electron density decrease with the increase of $|\kappa|$. Indeed, the ratio of the potential $|V|$ and the centrifugal term $|\kappa|/r$ in the Dirac equation decreases as $1/|\kappa|$. Therefore, to analyse the role of the corrections it is sufficient to consider the case of the minimal $|\kappa| = 1$, of s ($\kappa = -1$) and $p_{1/2}$ ($\kappa = 1$) waves. These are also the most important cases for the isotope shift.

The potential inside the nucleus $V = \frac{-Ze^2}{R} \left(\frac{3}{2} - \frac{r^2}{2R^2} \right)$ is quadratic and wave functions inside the nucleus correspond to the solutions for the relativistic oscillator. These solutions must be matched with the Coulomb solutions outside the nucleus¹. The result may be presented in the following form (see e.g. [13]):

$$\Psi_{s_{1/2}} = \begin{pmatrix} f_s \Omega_s \\ i g_s \Omega_{p_{1/2}} \end{pmatrix}, \quad (12)$$

$$\Psi_{p_{1/2}} = \begin{pmatrix} -\frac{A_p}{A_s} g_s \Omega_{p_{1/2}} \\ i \frac{A_p}{A_s} f_s \Omega_s \end{pmatrix}, \quad (13)$$

where f_s, g_s, A_s and A_s are defined in the Appendix A. As before, we treat the change in the potential within the nucleus due to the isotope effect (2) as our perturbation. Again, we find the energy shifts:

$$\delta\epsilon_s = \frac{3}{2} Z e^2 R^2 \frac{\delta R}{R} \int_0^1 (f_s^2 + g_s^2) (1-x^2) x^2 dx, \quad (14)$$

¹ These Coulomb solutions include regular and irregular at $r = 0$ components.

$$\delta\epsilon_{p_{1/2}} = \frac{3}{2} Z e^2 R^2 \left(\frac{A_p}{A_s} \right)^2 \frac{\delta R}{R} \times \int_0^1 (g_s^2 + f_s^2) (1-x^2) x^2 dx . \quad (15)$$

These expressions for the isotope shift are evaluated and expanded over small $Z^2\alpha^2$ to give

$$\delta\epsilon_s = \frac{1}{z_i + 1} \frac{1}{[\Gamma(2\gamma + 1)]^2} \left(\frac{2ZR}{a_b} \right)^{2\gamma} \frac{I_s^{3/2}}{Ry^{1/2}} \times \frac{4}{5} (1 - 0.24Z^2\alpha^2) \frac{\delta R}{R} , \quad (16)$$

$$\delta\epsilon_p = \frac{1}{z_i + 1} \frac{Z^2\alpha^2}{[\Gamma(2\gamma + 1)]^2} \left(\frac{2ZR}{a_b} \right)^{2\gamma} \frac{I_p^{3/2}}{Ry^{1/2}} \times \frac{1}{5} (1 + 0.26Z^2\alpha^2) \frac{\delta R}{R} . \quad (17)$$

Up to corrections $\pm 0.01Z^2\alpha^2$ these two expressions may be presented as one equation:

$$\delta\epsilon_{|\kappa|=1} = \frac{4}{5} \frac{1}{z_i + 1} \frac{\kappa(\kappa - \gamma)}{[\Gamma(2\gamma + 1)]^2} \times \left(\frac{2ZR}{a_b} \right)^{2\gamma} \frac{I^{3/2}}{(Ry)^{1/2}} \frac{\delta R}{R} . \quad (18)$$

One can see that the expression (18) directly follows from (11), if we put $|\kappa| = 1$. Estimates show that the higher order correction $\sim Z^4\alpha^4$ comes with a small coefficient.

Note that the ratio of the isotope shifts for $p_{1/2}$ and $s_{1/2}$ is equal to

$$\left(\frac{A_p}{A_s} \right)^2 = \left(\frac{I_p}{I_s} \right)^{3/2} \frac{z^2\alpha^2}{4} \left(1 + \frac{z^2\alpha^2}{4} \right)^2 \approx \left(\frac{I_p}{I_s} \right)^{3/2} \frac{1 - \gamma}{1 + \gamma}$$

III. NUMERICAL ESTIMATES FOR THE FIELD SHIFTS IN SUPERHEAVY ATOMS

Table I depicts the estimates for isotope shift in superheavy atoms which were calculated using Eq. (18). The ionization potentials used to calculate the field shift for each level in a given atom has been detailed in Appendix C. Furthermore, the nuclear radius R was found using $R = r_0 A^{1/3}$ where we assumed that $r_0 = 1.15$ fm for the purpose of these calculations.

One of the motivations for the current work was to provide a simple method to estimate IS which is suitable for superheavy atoms and provides a better understanding of its dependence on the nuclear and atomic parameters. Accurate many-body calculations of the field shift for No, Lr, Nh, Fl and Ra have recently been performed and presented in [5]. The CI+MBPT isotopic shift value for No

was found to be -7.28 cm $^{-1}$. Our approximate IS value for No is -9.2 cm $^{-1}$ as presented in Table I. The difference is actually comparable to 20% error of the CI+MBPT value.

The calculated IS for Lr, Nh and Fl is small due to large cancellations in the shifts between the lower p state and excited s state. We hence can provide only an order of magnitude estimates when calculating IS for transitions for $p \rightarrow s$ states using the method presented in this paper. Indeed, the $7p_{1/2}$ state IS is suppressed by the factor $(1 - \gamma)/(1 + \gamma)$ but enhanced by the higher $7p_{1/2}$ ionization potential than that of $8s$. This is why IS of $7p_{1/2}$ and $8s$ states nearly cancel each other out. While the absolute accuracy of IS calculations is the same, the relative accuracy of IS of the transition energy is poor. The value for the overall IS of Nh in our case is -0.35 cm $^{-1}$ which is significantly smaller than and opposite in sign to the CI+MBPT value for Nh which was stated to be 1.42 cm $^{-1}$. Similarly, we calculated an IS of -0.64 cm $^{-1}$ for Fl which is the same order of magnitude as CI+MBPT value given as 0.12 cm $^{-1}$ yet also opposite in sign. Our approximate value of IS for Lr is 0.78 cm $^{-1}$ which is notably smaller than the CI+MBPT value of 3.134 cm $^{-1}$. We re-iterate that the relative accuracies of the analytical formula and the CI+MBPT method in these cases are low, and all what we can conclude is that the IS is small and the frequencies of the transitions in all isotopes will be approximately the same.

We calculated field shifts of $s \rightarrow p$ transitions for several atoms and ions to compare with known experimental data. The results are presented in Tables II and III. The agreement for $s - p$ transitions is good. However, in the case of Ca^+ , formula (11) underestimates the measured field shifts of $3p^6 3d^2 D_{3/2} \rightarrow 3p^6 4p^2 P_{1/2}$ transition [14] by two orders of magnitude. The reason is that the direct field IS in $d - p$ transitions in light atoms is very small and the actual field IS is dominated by the core relaxation effect (the change of atomic potential due to the isotope shift in s -wave function) which will be discussed in the next section.

IV. NON-LINEARITIES IN KING PLOT FOR ISOTOPE SHIFTS

As we will show below the non-linear corrections to the King plot may be due to the non-factorization of the electronic and nuclear parameters in the expression for the field IS. This non-factorization appears if we have two or more nuclear parameters which are not proportional to each other and appear in different combinations for different atomic transitions.

As a rule, the second nuclear parameter gives a contribution to IS which is several orders of magnitude smaller than the contribution of the first nuclear parameter. This means that the non-linearity is small.

We do not consider here possible non-linearity effects which may, in principle, come from the mass IS (such as

Table I. Estimates of the isotope shift $\delta\nu$ for a given transition in superheavy atoms. A_1 is the atomic number of already synthesised reference isotope. $A_2 = Z + 184$ is the isotope of a given element belonging to the hypothetical island of stability with magic neutron number $N = 184$.

Atom		Transition		$\delta\nu$ (cm ⁻¹)	$\delta\nu$ (GHz)
Symbol	Z	A ₁	A ₂		
Cf	98	251	282	$5f^{10}7s^2 - 5f^{10}7s7p$	-7.6 -229
Es	99	252	283	$5f^{11}7s^2 - 5f^{11}7s7p$	-8.3 -248
Fm	100	257	284	$5f^{12}7s^2 - 5f^{12}7s7p$	-7.8 -233
Md	101	258	285	$5f^{13}7s^2 - 5f^{13}7s7p$	-8.4 -253
No	102	259	286	$7s^2 - 7s7p$	-9.2 -275
Lr	103	266	287	$7s^27p - 7s^28s$	0.78 23.3
Rf	104	263	288	$6d^27s^2 - 6d^27s7p$	-10 -300
Db	105	268	289	$6d^37s^2 - 6d^37s7p$	-9.1 -274
Sg	106	269	290	$6d^47s^2 - 6d^47s7p$	-9.9 -298
Bh	107	270	291	$6d^57s^2 - 6d^57s7p$	-11 -325
Hs	108	269	292	$6d^67s^2 - 6d^67s7p$	-13 -389
Mt	109	278	293	$6d^77s^2 - 6d^77s7p$	-9.2 -275
Ds	110	281	294	$6d^87s^2 - 6d^87s7p$	-8.7 -260
Rg	111	282	295	$6d^97s^2 - 6d^97s7p$	-9.5 -285
Cn	112	285	296	$6d^{10}7s^2 - 6d^{10}7s7p$	-8.8 -263
Nh	113	286	297	$7s^27p - 7s^28s$	-0.35 -10.5
Fl	114	292	298	$7p^2 - 7p8s$	-0.64 -19.3

contributions of the relativistic and quadratic effects in the mass IS).

A. King plot in the mean field (single-particle) approximation

With $\mu_{AA'} = \frac{1}{m_A} - \frac{1}{m_{A'}}$, where the masses of isotopes A and A' are denoted as m_A and $m_{A'}$ respectively, the IS can be written as follows:

$$\nu_i^{AA'} = K_i \mu_{AA'} + F_i \delta \langle r^{2\gamma_1} \rangle_{AA'} + G_i \delta \langle r^{2\gamma_2} \rangle_{AA'} . \quad (19)$$

The first term expresses the mass shift (both normal and specific). The second term is the leading-order contribution to the field shift discussed in the previous sec-

Table II. Comparison of experimental field shifts in Ca, Yb and Hg with theoretical prediction based on formula (11) and experimental values of mean nuclear charge radii. Both measured field shifts and nuclear charge radii are found in [15].

Atom	A ₁	A ₂	Transition	$\Delta\nu_{\text{exper}}$ (MHz)	$\Delta\nu_{\text{theor}}$ (MHz)
Ca	46	48	$3p^64s^2 - 3p^64s4p$	-25.3 ± 1.0	-31
Yb	174	176	$4f^{14}6s^2 - 4f^{14}6s6p$	993 ± 250	1217
Hg	202	204	$5d^{10}6s^2 - 5d^{10}6s6p$	5238 ± 11	4939

Table III. Comparison of experimental field shifts for the $3p^64s \ ^2S_{1/2} \rightarrow 3p^64p \ ^2P_{1/2}$ transition in Ca⁺ [14] with theoretical results using formula (11) and nuclear charge radii data from [15].

	MHz		
	$\delta\nu_{\text{field}}^{40, 42}$	$\delta\nu_{\text{field}}^{40, 44}$	$\delta\nu_{\text{field}}^{40, 48}$
Theory	-61.0	-81.1	8.27
Exp.	-60.9	-79.6	1.27

tion. For s -wave in the non-relativistic limit ($\gamma_1 \rightarrow 1$) this term scales with the difference of mean squares of nuclear charge radii between the isotopes A and A' : $\delta \langle r^2 \rangle_{AA'}$. The third term expresses a correction to the field shift produced by higher waves. For example, for $p_{3/2}$ in the non-relativistic limit, $\gamma_2 \rightarrow 2$ and $\delta \langle r^{2\gamma_2} \rangle_{AA'} = \delta \langle r^4 \rangle_{AA'}$. A similar term may appear as a sub-leading correction to the s -wave field shift but it does not produce a contribution to the non-linearity of the King plot since it only redefines the the main s - wave contribution $F_i \delta \langle r^{2\gamma_1} \rangle_{AA'}$, i.e. it produces a correction which is the same in different atomic transitions. The non-linearity appears when the ratio G_i/F_i changes (see below).

Next we divide equation (19) through by $\mu_{AA'}$ and hence define a new modified frequency $n_i = \nu_i^{AA'}/\mu_{AA'}$:

$$n_i = K_i + F_i x + G_i y, \quad (20)$$

with $x = \delta \langle r^{2\gamma_1} \rangle_{AA'} / \mu_{AA'}$ and $y = \delta \langle r^{2\gamma_2} \rangle_{AA'} / \mu_{AA'}$. Here $i = 1, 2$ are the two transitions examined in a chain of isotopes. A plot of n_1 vs. n_2 gives what is known as a King plot [16]. If we assume $G_{1,2} = 0$, one can write n_2 as a linear function of n_1 , i.e. the King plot is linear. To trace the possible non-linearity, we must consider at least 4 isotopes (A, A_1, A_2, A_3) forming 3 pairs, giving three points on the plot:

$$AA_1 \equiv a, \quad AA_2 \equiv b, \quad AA_3 \equiv c. \quad (21)$$

The first two points can be used to determine the gradient $k = (n_2^b - n_2^a) / (n_1^b - n_1^a)$. Let us state a hypothetical \tilde{c} point, lying on the same line as a and b :

$$n_2^{\tilde{c}} = n_2^b + k(n_1^c - n_1^b). \quad (22)$$

Then the non-linearity is indicated by the difference (see Fig. 1):

$$n_2^c - n_2^{\tilde{c}} = K_2 + F_2 x^c + G_2 y^c - K_2 - F_2 x^b - G_2 y^b - \frac{F_2(x_b - x_a) + G_2(y_b - y_a)}{F_1(x_b - x_a) + G_1(y_b - y_a)} [F_1(x_c - x_b) + G_1(y_c - y_b)].$$

Under the assumption of $\frac{G\Delta y}{F\Delta x} \ll 1$ and with $q_{ba} \equiv \frac{y_b - y_a}{x_b - x_a}$, one can show that:

$$n_2^c - \tilde{n}_2^c = (x_c - x_b)(q_{cb} - q_{ba}) \left(\frac{G_2}{F_2} - \frac{G_1}{F_1} \right) F_2. \quad (23)$$

Here we see that the non-linear correction vanishes in two cases:

1. $q_{cb} = q_{ba}$,

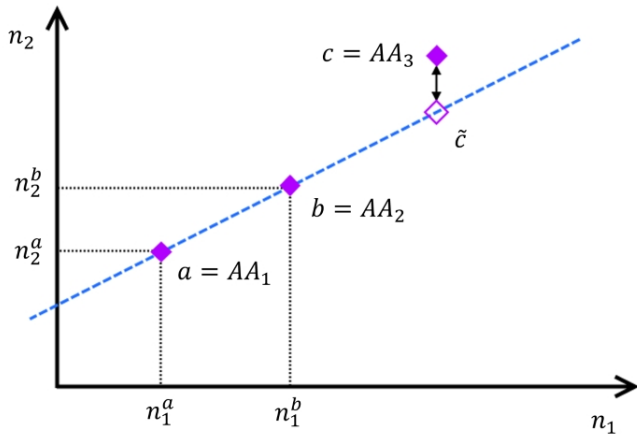


Figure 1. Schematic illustration of the King plot non-linearity. Modified frequencies n_1 and n_2 are plotted for the three pairs of isotopes (21). The difference between point c and hypothetical point \tilde{c} lying on the same line as a and b leads to the evaluation of non-linearity of the plot.

$$2. \frac{G_2}{F_2} = \frac{G_1}{F_1}.$$

The first case considers $\delta \langle r^{2\gamma_1} \rangle$ and $\delta \langle r^{2\gamma_2} \rangle$. These parameters are correlated: generally speaking, increase of the nuclear radius R leads to the increase of both $\delta \langle r^{2\gamma_1} \rangle$ and $\delta \langle r^{2\gamma_2} \rangle$. It is easy to check that if the field shift for all isotopes is completely defined by the change of the nuclear radius δR from isotope to isotope, i.e. if $\delta \langle r^{2\gamma} \rangle = D_\gamma \delta R$ for any δR (as in the linear approximation in δR), we have $q_{cb} = q_{ba}$.

For example, in the isotope shift (11) the dependence on R is given by $R^{2\gamma-1} \delta R$ and the difference between two isotopes is proportional to $R_A^{2\gamma-1} \delta R_{A\tilde{A}}$. This, given fixed reference isotope A , leads to $q_{cb} = q_{ba}$. Therefore, to get a non-zero result we should go beyond the first order in $\delta R/R$. We integrate formula (11) to effectively include all orders of perturbation theory in $\delta R/R$. Then the field shift of an energy level between isotopes A and \tilde{A} is:

$$\Delta \epsilon_{\kappa, A\tilde{A}} = \frac{12\kappa(\kappa - \gamma)}{2\gamma(z_i + 1)(2|\kappa| + 1)(2|\kappa| + 3)[\Gamma(2\gamma + 1)]^2} \times \left(\frac{2Z}{a_b} \right)^{2\gamma} \frac{I^{3/2}}{Ry^{1/2}} \left(R_{\tilde{A}}^{2\gamma} - R_A^{2\gamma} \right). \quad (24)$$

We plot the field shifts of transition frequencies $(\Delta \epsilon_{\kappa(up)} - \Delta \epsilon_{\kappa(down)})_{A\tilde{A}}$ for three pairs of isotopes of four elements: Ca^+ , Sr^+ , Yb^+ and Hg^+ . Fitting a line to the first two pairs a and b , we find the nonlinearity as $(n_2^c - \tilde{n}_2^c) \mu_c$.

The results are presented in Table IV. In order to find the radii R for substituting into (24), we first make use of the simple liquid-drop model where $R = r_0 A^{1/3}$ (Method 1 in Table IV). Then to obtain more realistic estimate we find equivalent R from the experimental values of mean square nuclear charge radius [15] (Method 2 in Table IV): $R^2 = \frac{5}{3} \langle r^2 \rangle$.

The expression (24) is, in fact, only the first order contribution to the field shift in terms of energy. The second order in the single-electron approximation can be roughly estimated as a quadratic term $\pm (\Delta \epsilon_{\kappa, A\tilde{A}})^2 / I$. Due to its smallness in higher waves ($\kappa \neq -1$) it has only a negligible effect on the King plot non-linearity. But, as will be shown in Sec. IV C, if we include many-body corrections, this quadratic term can alter considerably the non-linearity value in heavy atoms (the field shift is $\propto Z^{2\gamma}$, correspondingly the quadratic term is $\propto Z^{4\gamma}$).

B. Nuclear polarizability effect

The nuclear structure effects for simple atoms have been considered in Ref. [17]. We are interested in such effects in many-electron atoms. The nuclear polarization potential produced by the nuclear polarizability α_E is a long-range one ($V_\alpha = -\frac{1}{2} \frac{\alpha_E e^2}{r^4}$), therefore it can give a significant contribution to a higher-wave isotope shift and overall non-linearity of King plot. The main contribution to the corresponding energy shift comes from the

area near the nucleus where the nuclear potential is not screened. In order to estimate the shift, we integrate the radial density $\rho_\kappa = f_\kappa^2 + g_\kappa^2$ using atomic wave functions proportional to the Coulomb wave functions outside the nucleus (see Appendix B) with the interaction Hamiltonian V_α .

$$\delta\epsilon_E = \int_{r_0}^{+\infty} (f_\kappa^2(r) + g_\kappa^2(r)) \left(-\frac{1}{2} \frac{\alpha_E e^2}{r^4} \right) r^2 dr, \quad (25)$$

$$r_0 = \begin{cases} R & , |\kappa| = 1, \\ 0 & , |\kappa| > 1. \end{cases}$$

For $|\kappa| > 1$ the integral with the Coulomb wave functions converges at $r = 0$ and we may calculate it taking the cut-off parameter $r_0 = 0$. In this case a general analytic solution is relatively simple and can be presented here as:

$$\delta\epsilon_E = -\alpha_E \frac{9 + 5\kappa(\kappa - 3) + 5Z^2\alpha^2 + \gamma^2}{256\gamma(-9 + \gamma^2(7 - 4\gamma^2)^2)} \times \frac{8^3 Z^2}{a_b^3} \frac{2}{z_i + 1} \frac{I^{3/2}}{Ry^{1/2}}, \quad (26)$$

where $\gamma = \sqrt{\kappa^2 - Z^2\alpha^2}$ and I is the ionization potential of the electron, a_b the Bohr radius, Ry the Rydberg constant and z_i the ion charge. For $|\kappa| = 1$, the integral in Eq. (25) from 0 would diverge, but a cut-off from nuclear radius R would give a reasonable estimate of the effect. Note that s orbital always appears in both transitions which we compare in the King plot, therefore the exact magnitude of this $|\kappa| = 1$ term is not important for the estimate of the non-linearity.

To obtain the numerical values for the integral with $|\kappa| = 1$ we have used the Bessel function solutions from Appendix B, however, without loss of the actual numerical accuracy its adequate approximation can be found by substituting expressions for wave functions expanded at $r \rightarrow 0$ (see Appendix C) to the integral (25):

$$\delta\epsilon_E = -\alpha_E \frac{8\kappa(\kappa - \gamma)}{3 - 2\gamma} \frac{1}{z_i + 1} \frac{Z}{a_b^2} \times \frac{1}{[\Gamma(2\gamma + 1)]^2} \left(\frac{a_b}{2Z} \right)^{2-2\gamma} \frac{I^{3/2}}{Ry^{1/2}} R^{2\gamma-3}. \quad (27)$$

An expression for nuclear polarizability α_E based on the giant resonance approach was obtained by Migdal [18, 19]:

$$\alpha_E = \frac{e^2 R^2 A}{40 a_{sym}}. \quad (28)$$

We use the empirical value of the nuclear symmetry energy $a_{sym} = 23$ MeV [20, 21]. To the first order one can treat the change of α_E as consisting of two independent parts, one resulting from the growth of nuclear radius ΔR and another from the change of nucleon number ΔA :

$$\Delta\alpha_E = \frac{2e^2 R}{40 a_{sym}} A \Delta R + \frac{e^2 R^2}{40 a_{sym}} \Delta A. \quad (29)$$

The second contribution can be independently evaluated using the nuclear oscillator model. From the second-order perturbation theory follows that with the addition of one neutron, the nuclear polarizability changes as:

$$\delta\alpha = -q_n^2 \left[\frac{\langle n|x|n+1 \rangle^2}{E_n - E_{n+1}} + \frac{\langle n|x|n-1 \rangle^2}{E_n - E_{n-1}} \right] \quad (30)$$

Here $q_n = eZ/A$ is the effective charge of a neutron, originating from the recoil effect². Energy levels of a quantum oscillator are known to be $E_n = \hbar\omega(n + \frac{1}{2})$ and its matrix elements can be written [22]:

$$\langle n|x|n+1 \rangle^2 = \frac{(n+1)\hbar}{2M\omega}, \quad \langle n|x|n-1 \rangle^2 = \frac{n\hbar}{2M\omega},$$

with the frequency $\omega = (40 \text{ MeV})/(\hbar A^{1/3})$ for the case of nuclei and M being neutron mass. Assuming here $R = r_0 A^{1/3}$, one can express:

$$\omega = \frac{40 \text{ MeV } r_0}{\hbar R},$$

$$\begin{aligned} \Delta\alpha_{E,A} &= \delta\alpha \Delta A = \frac{e^2}{2M\omega^2} \left(\frac{Z}{A} \right)^2 \Delta A \\ &= \frac{e^2 \hbar^2}{2M} \left(\frac{Z}{A} \right)^2 \left(\frac{R}{r_0 \times (40 \text{ MeV})} \right)^2 \Delta A. \end{aligned} \quad (31)$$

The second term in (29) and (31) are close in value and they both depend on R^2 . It means that the formula (28) effectively includes the contribution from adding neutrons and we can use it alone to estimate the change of nuclear polarizability between isotopes. We introduce empirical coefficient $\zeta(A)$ to scale our prediction to the more accurately evaluated nuclear polarizabilities in [23].

$$\zeta(A) = 0.76 + \frac{2.79}{A^{1/3}},$$

$$\alpha_E = \zeta(A) \frac{e^2 R^2 A}{40 a_{sym}}. \quad (32)$$

This final expression of nuclear polarizability is used to model the King plot non-linearity, which grows dramatically compared to the non-linearity found only according to the field shift formula (24), as can be seen in Table IV.

² The second term with the matrix element $\langle n|x|n-1 \rangle$ obviously appears within the single-particle consideration. On the many-body language it is the "blocking" contribution: core neutrons can not be excited to the state occupied by the valence neutron.

Table IV. Estimates for the non-linearities of King plot. Methods 1 and 2 are based on the single-electron analytic expression of field isotope shift (24) found from the estimate of wave function density (9) in an uniformly charged spherical nucleus. Method 1 utilizes the liquid drop approximation for nuclear radius $R = r_0 A^{\frac{1}{3}}$ with $r_0 = 1.15$ fm and Method 2 uses experimental data [15] for mean squares of nuclear charge radii $\langle r^2 \rangle$ when finding the equivalent nuclear radius: $\langle r^2 \rangle = \frac{2}{5} R^2$. Method 3 accounts for both expression (24) and the contribution of nuclear polarizability (25), equivalent nuclear radius R is again based on the experimental data.

Ion	Pair of transitions					Non-linearity (Hz)			
	Z	A	A ₁	A ₂	A ₃	Method 1	Method 2	Method 3	
Ca ⁺	20	40	42	44	48	$3p^6 4s \ ^2S_{1/2} \rightarrow 3p^6 4p \ ^2P_{1/2}$	-1.2×10^{-4}	1.6×10^{-4}	–
						$3p^6 3d \ ^2D_{3/2} \rightarrow 3p^6 4p \ ^2P_{1/2}$			
						$3p^6 4s \ ^2S_{1/2} \rightarrow 3p^6 3d \ ^2D_{3/2}$	-1.2×10^{-4}	1.6×10^{-4}	-4.1×10^{-2}
						$3p^6 4s \ ^2S_{1/2} \rightarrow 3p^6 3d \ ^2D_{5/2}$			
Sr ⁺	38	84	86	87	88	$4p^6 5s \ ^2S_{1/2} \rightarrow 4p^6 4d \ ^2D_{3/2}$	4.5×10^{-4}	-1.7×10^{-3}	1.7×10^{-1}
						$4p^6 5s \ ^2S_{1/2} \rightarrow 4p^6 4d \ ^2D_{5/2}$			
Yb ⁺	70	168	170	172	176	$4f^{14} 6s \ ^2S_{1/2} \rightarrow 4f^{13} 6s^2 \ ^2F_{7/2}^o$	6.1×10^{-2}	–3.1	38
						$4f^{14} 6s \ ^2S_{1/2} \rightarrow 4f^{14} 5d \ ^2D_{3/2}$			
						$4f^{14} 6s \ ^2S_{1/2} \rightarrow 4f^{14} 5d \ ^2D_{3/2}$	-6.1×10^{-2}	3.1	–18
						$4f^{14} 6s \ ^2S_{1/2} \rightarrow 4f^{14} 5d \ ^2D_{5/2}$			
Hg ⁺	80	196	198	200	204	$5d^{10} 6s \ ^2S_{1/2} \rightarrow 5d^9 6s^2 \ ^2D_{3/2}$	5.5×10^{-1}	3.1	–14
						$5d^{10} 6s \ ^2S_{1/2} \rightarrow 5d^9 6s^2 \ ^2D_{5/2}$			

C. Many-body corrections

The results above have been obtained in the single-particle mean field approximation. However, the isotope shifts in all waves with $|\kappa| > 1$ are dominated by the many-body effects. The change of the isotope changes s wave electron wave functions. This produces the correction δV to the electron potential which gives the dominating contribution to the isotope shifts of the orbitals with $|\kappa| > 1$ (the core relaxation effect). Therefore, in any wave the dominating term in the isotope shift is proportional to $\delta \langle r^{2\gamma_1} \rangle_{AA'}$, corresponding to $|\kappa| = 1$. However, the term with $\delta \langle r^{2\gamma_2} \rangle_{AA'}$, still appears in the transition frequencies and the logic of the section above does not change. The many-body corrections only affect the magnitude of the coefficients F_i and G_i in the isotope shift Eq. (19).

Consider, for example, King plot for $s - d_{3/2}$ and $s - d_{5/2}$ transitions for Ca⁺, Sr⁺ and Yb⁺ presented in the Table IV. Firstly, there are higher order terms in the expansion of the s -wave density near origin, $\sim r^{2\gamma_1+2}$. They only lead to the redefinition of the main term $\delta \langle r^{2\gamma_1} \rangle_{AA'}$ and do not produce any new physical effects. The core relaxation effect and other many-body corrections for s orbital are relatively small, $\sim 10 - 20\%$ and give contributions to the coefficient F_i which are the same for both transitions and therefore insignificant. The core relaxation effects for $d_{3/2}$ and $d_{5/2}$ are huge in comparison with the direct contributions but their absolute values are smaller than that for $s_{1/2}$. These core relaxation effects produce some corrections to the coefficients F_i and

G_i but do not give a significant contribution to the non-linearity of the King plot. This non-linearity comes from the direct contribution to the term $G_i \delta \langle r^{2\gamma_2} \rangle_{AA'}$, since the density of $d_{3/2}$ orbital ($\kappa = 2$) near nucleus is several orders of magnitude larger than the density of $d_{5/2}$ orbital ($\kappa = -3$). We have already taken this effect into account at the single-particle level. The IS correction to the potential δV is located at larger distances where the densities of $d_{3/2}$ and $d_{5/2}$ are approximately the same.

The nonlinear corrections may be significantly larger in atoms with several valence electrons. The density of energy levels is much higher in such systems. In this case the second order effects in the field shift perturbation δV in Eq. (2) may be enhanced by small energy denominators and produce large non-linear effects in the King plot [24–28].

We want to provide a rough numerical estimate of the many-body effects to the non-linearity of the King plot using a simple model. From our experience we know that the many-body correction to the s -wave field shift is ~ 10 times smaller than the single-particle shift. Therefore we model the core relaxation effect by the following expression: $\Delta \varepsilon_s - \frac{\Delta \varepsilon_s}{10}$. Here the initial $\Delta \varepsilon_s = \Delta \varepsilon_s + \delta \varepsilon_{E,s}$ comprises both single-electron contribution (24) and the polarizability term (27). Non-linear corrections to the King plot may also be produced by the quadratic effects in the field shift, which we further estimate as $\pm (\Delta \varepsilon_s - \frac{\Delta \varepsilon_s}{10})^2 / I_s$.³ Therefore the complete formulae

³ The quadratic effect may be enhanced if there is a close atomic

Table V. Estimates for the non-linearities of King plot, taking into account the many-body core relaxation corrections, as shown in (33) – (36). Method 4 is based on a sum of the single-electron analytically determined contribution (24) and the first-order many-body effect ($-\Delta\varepsilon_\kappa/10$). Method 5 uses the single-electron term (24), the first-order many-body effect and the polarizability contribution (25). The last two columns show the second-order contributions to the non-linearity with an unknown sign arising from the quadratic terms (e.g. (34) and (36)). The third column shows the quadratic corrections ignoring the nuclear polarizability α_E , i.e. it corresponds to Method 4. The second-to-last column takes into account the polarizability contribution and thus corresponds to Method 5. The last column details the nonlinearity due to the quadratic mass shift (QMS) estimated from the normal mass shift contribution as presented in (38).

Ion	Pair of transitions					Non-linearity (Hz)					
	Z	A	A ₁	A ₂	A ₃	Method 4	Method 5	Quadratic term inc. MB		QMS	
								without α_E	with α_E		
Ca ⁺	20	40	42	44	48	$3p^6 4s \ ^2S_{1/2} \rightarrow 3p^6 3d \ ^2D_{3/2}$ $3p^6 4s \ ^2S_{1/2} \rightarrow 3p^6 3d \ ^2D_{5/2}$	1.6×10^{-4}	-4.0×10^{-2}	$\pm 2.5 \times 10^{-4}$	$\pm 2.2 \times 10^{-4}$	± 1.4
Sr ⁺	38	84	86	87	88	$4p^6 5s \ ^2S_{1/2} \rightarrow 4p^6 4d \ ^2D_{3/2}$ $4p^6 5s \ ^2S_{1/2} \rightarrow 4p^6 4d \ ^2D_{5/2}$	-1.7×10^{-3}	1.7×10^{-1}	$\mp 5.7 \times 10^{-3}$	$\mp 5.8 \times 10^{-3}$	∓ 0.54
Yb ⁺	70	168	170	172	176	$4f^{14} 6s \ ^2S_{1/2} \rightarrow 4f^{13} 6s^2 \ ^2F_{7/2}^o$ $4f^{14} 6s \ ^2S_{1/2} \rightarrow 4f^{14} 5d \ ^2D_{3/2}$ $4f^{14} 6s \ ^2S_{1/2} \rightarrow 4f^{14} 5d \ ^2D_{3/2}$ $4f^{14} 6s \ ^2S_{1/2} \rightarrow 4f^{14} 5d \ ^2D_{5/2}$	-3.1	38	± 2124	± 2096	± 30
Hg ⁺	80	196	198	200	204	$5d^{10} 6s \ ^2S_{1/2} \rightarrow 5d^9 6s^2 \ ^2D_{3/2}$ $5d^{10} 6s \ ^2S_{1/2} \rightarrow 5d^9 6s^2 \ ^2D_{5/2}$	3.0	-14	± 406	± 402	± 0.43

for the shift of an energy level will look as:

$$\Delta\tilde{\varepsilon}_s = \Delta\varepsilon_s - \frac{\Delta\varepsilon_s}{10}, \quad (33)$$

$$\Delta\tilde{\tilde{\varepsilon}}_s = \Delta\tilde{\varepsilon}_s \pm \frac{(\Delta\tilde{\varepsilon}_s)^2}{I_s}. \quad (34)$$

For the higher waves δV is dominated by the corrections to the s -wave functions. Here $\Delta\varepsilon_\kappa$ again consists of both contributions (24) and (26).

$$\Delta\tilde{\varepsilon}_\kappa = \Delta\varepsilon_\kappa - \frac{\Delta\varepsilon_{s,\kappa}}{10}, \quad \Delta\varepsilon_{s,\kappa} = \Delta\varepsilon_s \left(\frac{I_\kappa}{I_s} \right)^{3/2}, \quad (35)$$

$$\Delta\tilde{\tilde{\varepsilon}}_\kappa = \Delta\tilde{\varepsilon}_\kappa \pm \frac{(\Delta\tilde{\varepsilon}_\kappa)^2}{I_\kappa}. \quad (36)$$

I_s denotes the ionization potential of an s -wave, I_κ of any other wave.

King plot non-linearity values taking into account many-body contributions are presented in Table V. As can be seen, the addition of the first order corrections (33) and (35) indeed does not considerably affect the non-linearity⁴.

On the other hand, the quadratic terms (34) and (36) are responsible for the radical growth of King plot non-linearity in heavy atoms (especially for f -shell transition in Yb⁺), while remaining insignificant in Ca⁺ and Sr⁺. Indeed, the field shift is $\propto Z^{2\gamma}$, correspondingly the quadratic term is $\propto Z^{4\gamma}$, i.e. it very rapidly increases with the nuclear charge.

V. ESTIMATE OF THE QUADRATIC MASS SHIFT IN THE KING PLOT NON-LINEARITY

For a rough estimate we only consider the contribution of the normal mass shift:

$$\Delta\varepsilon_M = -\varepsilon m_e \mu_{AA'} \quad (37)$$

$$\Delta\tilde{\tilde{\varepsilon}}_{M2} = \pm \frac{(\Delta\varepsilon_M)^2}{I}, \quad (38)$$

where m_e is the electron mass. The non-linearity of the King plot arising from the addition of terms (37) and (38) to the IS is shown in the last column of Table V.

one must include all effects which have been included at the single-particle level. For example, if the field shift term (24) and the nuclear polarizability contribution (27) have been included at the single-particle level they both must be included in the core polarization effect. If it contains only the first term, the resulting first and second order many-body effects will generate a large phantom non-linearity in the King plot, because the dependence on the nuclear parameters (radius R and mass number A) is no longer the same for the single-electron and many-body effect.

level with the same angular momenta and parity which may be admixed by the IS operator. This does not happen in atoms with one electron above close shells which we consider.

⁴ It should be noted that for the evaluation of many-body effects

VI. NEW PARTICLE

King plot non-linearity may arise as a result of an interaction between electrons and neutrons mediated by a new particle of mass m_ϕ [29]. The effective potential associated with such a particle would be the Yukawa potential:

$$V_\phi(r) = -q_n q_e N \frac{e^{-kr}}{r}, \quad (39)$$

$$k = \frac{m_\phi c}{\hbar}, \quad \alpha_{\text{NP}} = q_n q_e,$$

here N is the neutron number, q_n and q_e are particle coupling strengths to the neutrons and electrons respectively, r is the distance from the nucleus. We aim at constraining the coupling constant α_{NP} . Let us estimate the energy shifts in atomic states that the new particle might cause. When the particle is very light ($k \ll 1/a_b$) and therefore $e^{-kr} \approx 1$, the potential (39) becomes Coulomb-like:

$$V_\phi(r) = -q_n q_e N \frac{1}{r}. \quad (40)$$

Making use of the virial theorem, one can express the average potential energy of the system as double total energy:

$$\langle V \rangle = 2E_{\text{tot}}. \quad (41)$$

Substituting here values for a single outer electron in the Coulomb field $V = V_c = -(z_i + 1)e^2/r$ and $E_{\text{tot}} = -I_\kappa$, one obtains:

$$\left\langle \frac{1}{r} \right\rangle = \frac{2I_\kappa}{(z_i + 1)e^2}. \quad (42)$$

Therefore the energy shift of an electron with a given κ arising from a new light particle, seen as the change of $\langle V_\phi \rangle$ between the isotopes, can be approximately written as:

$$\Delta\epsilon_{\phi,\kappa} = -\frac{q_n q_e}{e^2} \frac{2I_\kappa}{(z_i + 1)} \Delta N \quad (43)$$

On the other hand, the energy shifts resulting from an interaction mediated by heavier particles ($Z^{1/3}/a_b < k < 1/R$, here R is the nuclear radius, and $a_b/Z^{1/3}$ is the Thomas-Fermi electron screening radius) are found by direct integration of (39) with the relativistic wave functions for a valence electron (see Appendix B):

$$\Delta\epsilon_{\phi,\kappa} = -q_n q_e \Delta N \int_0^\infty (f_\kappa^2(r) + g_\kappa^2(r)) \frac{e^{-kr}}{r} r^2 dr. \quad (44)$$

For larger masses, $Z/a_b < k < 1/R$, it is instructive to present also approximate formula for (44) which shows

dependence on the Compton wavelength $k = \frac{m_\phi c}{\hbar}$ and other parameters explicitly:

$$\Delta\epsilon_{\phi,\kappa} = -\frac{q_n q_e}{e^2} \frac{4\kappa(\kappa - \gamma)}{(z_i + 1)Z} \frac{\Gamma(2\gamma)}{[\Gamma(2\gamma + 1)]^2} \left(\frac{2Z}{ka_b} \right)^{2\gamma} \times \frac{I_\kappa^{3/2}}{Ry^{1/2}} \Delta N. \quad (45)$$

The effect of very heavy bosons with $k > 1/R$ is absorbed into the usual field shift (proportional to $R^{2\gamma}$), as the range of the interaction is less than the nuclear radius. It is therefore nearly impossible to see this new physics effect against the background of nuclear uncertainties. We restrict our consideration with masses corresponding to $k < 1/R$, i.e. $m_\phi \lesssim 30$ MeV.

As always, the IS of a transition frequency would be the difference of the shifts of two levels $\Delta\epsilon_{\phi,\kappa}$. We examine the non-linearity arising from the addition of these terms to otherwise linear King plot which we construct leaving only the s-wave contribution of the form (24) in all transitions. We also take into account the characteristic value of many-body core relaxation corrections. Then we examine the sensitivity of non-linearity to the coupling constant $\frac{q_n q_e}{e^2}$ by equating the non-linearity which appears as a result of including a new particle and the non-linearity emerging naturally from SM. The values of $\frac{q_n q_e}{e^2}$ that lead to the same non-linearity as SM corrections in a given pair of transitions are presented in Table VI.

VII. CONCLUSIONS

The analytical formula for the field isotope shift Eq. (11) gives reasonable accuracy of the estimates for the transitions involving s-wave electron. In superheavy elements it should also describe the $p_{1/2}$ -wave field IS which is comparable to the s-wave shift. For higher waves the field IS is dominated by the many-body corrections which are dominated by the core relaxation effect produced by the IS of the mean field potential due to IS of the s-wave electron wave functions.

In the single-particle mean-field approximation the non-linearity of the King plot is strongly dominated by the nuclear polarizability contribution - see Table IV. However, the quadratic field shift, which very rapidly increases with the nuclear charge Z and gives the dominating contribution to the non-linearity of the King plot in heavy atoms, is not so sensitive to the nuclear polarizability contribution - see Table V. However, in medium atoms the quadratic terms are not so large, therefore, the measurements of the non-linearity of the King plot may, in principle, be used to extract the nuclear polarizability differences between the isotopes.

Contribution of the new particle increases with the nuclear charge Z . However, the quadratic contribution to the field IS increases with Z much faster. In light atoms the non-linearity is dominated by the quadratic mass

Table VI. Values of the ratio $q_n q_e / e^2$ of the product of the coupling constants $q_n q_e$ for a new particle of a mass m_ϕ to the squared electron electric charge e^2 . It corresponds to the most significant King plot non-linearity value that can arise from SM corrections to the IS (see Table V). Individual isotope shifts consist of the s -wave contribution, which does not give rise to any non-linearity, and the new particle contributions (43) and (44) for light ($m_\phi \rightarrow 0$) and heavier particles respectively.

Ion	Pair of transitions					Non-linearity (Hz)	Non-linearity $\frac{q_n q_e}{e^2}$					
	Z	A	A ₁	A ₂	A ₃		$m_\phi \rightarrow 0$	$m_\phi = 10^5$ eV	$m_\phi = 10^6$ eV	$m_\phi = 10^7$ eV		
Ca ⁺	20	40	42	44	48	$3p^6 4s \ ^2S_{1/2} \rightarrow 3p^6 3d \ ^2D_{3/2}$	-1.4	8.7×10^{-12}	5.7×10^{-10}	1.4×10^{-6}	-1.4×10^{-2}	
						$3p^6 4s \ ^2S_{1/2} \rightarrow 3p^6 3d \ ^2D_{5/2}$						
Sr ⁺	38	84	86	87	88	$4p^6 5s \ ^2S_{1/2} \rightarrow 4p^6 4d \ ^2D_{3/2}$	0.7	1.0×10^{-12}	3.2×10^{-11}	2.6×10^{-8}	1.9×10^{-4}	
						$4p^6 5s \ ^2S_{1/2} \rightarrow 4p^6 4d \ ^2D_{5/2}$						
Yb ⁺	70	168	170	172	176	$4f^{14} 6s \ ^2S_{1/2} \rightarrow 4f^{13} 6s^2 \ ^2F_{7/2}^o$	2164	-4.9×10^{-12}	2.0×10^{-9}	9.3×10^{-7}	-1.5×10^{-1}	
						$4f^{14} 6s \ ^2S_{1/2} \rightarrow 4f^{14} 5d \ ^2D_{3/2}$						
						$4f^{14} 6s \ ^2S_{1/2} \rightarrow 4f^{14} 5d \ ^2D_{3/2}$						-79.0
						$4f^{14} 6s \ ^2S_{1/2} \rightarrow 4f^{14} 5d \ ^2D_{5/2}$						
$5d^{10} 6s \ ^2S_{1/2} \rightarrow 5d^9 6s^2 \ ^2D_{3/2}$	-416.4	-3.4×10^{-11}	2.2×10^{-9}	3.7×10^{-7}	1.3×10^{-3}							
$5d^{10} 6s \ ^2S_{1/2} \rightarrow 5d^9 6s^2 \ ^2D_{5/2}$												

shift. Therefore, it may be easier to extract a competitive limit on the new particle interaction strength from the measured non-linearity of the King plot in medium atom transitions such as $s-d$ transitions in Sr⁺ and Yb⁺ - see Table VI.

The field IS may be an order of magnitude smaller in transitions which do not involve s -wave electrons. This means that the dominating source of the King plot non-linearity in heavy atoms, the quadratic field IS term, may be two orders of magnitude smaller. Such transitions may, in principle, provide two orders of magnitude better accuracy for the low mass new particle. However, these must be transitions with a small natural width. In all existing optical atomic clocks such narrow transitions always involve s -electron. Therefore, to explore such possibility we should look for narrow transitions in atoms and ions containing p , d or f electrons in the ground open shell, or low energy excitations from the closed f , d , p shells.

VIII. ACKNOWLEDGEMENTS

This work was supported by the Australian Research Council and the Gutenberg Fellowship. The authors are grateful to S. Karshenboim, K. Pachucki, M. Pospelov, D. Budker and V. Shabaev for valuable discussions. A.V.V. would like to thank UNSW, Australia for hospitality.

APPENDIX

A. Relativistic electron wave function inside nucleus

The s and $p_{1/2}$ approximate wave functions within the nucleus in a neutral atom are presented in [13, 30]. We have introduced minor changes to extend the result to ions with charge z_i . Denoting $x = r/R$, the upper and lower radial components of the s wave function can be given:

$$f_s = A_s \left[1 - \frac{3}{8} Z^2 \alpha^2 x^2 \left(1 - \frac{4}{15} x^2 \right) \right], \quad (46)$$

$$g_s = -\frac{1}{2} A_s Z \alpha x \times \left[1 - \frac{1}{5} x^2 - \frac{9}{40} Z^2 \alpha^2 x^2 \left(1 - \frac{3}{7} x^2 + \frac{4}{81} x^4 \right) \right], \quad (47)$$

Where A_s is a constant defined as

$$A_s = \frac{2}{(z_i + 1)^{1/2}} \frac{2 \left(\frac{a_b}{2ZR} \right)^{1-\gamma}}{\Gamma(2\gamma + 1)} \left(\frac{Z}{a_b^3} \right)^{1/2} \times \left(\frac{I}{Ry} \right)^{3/4} \left(1 - \frac{1}{40} Z^2 \alpha^2 \right). \quad (48)$$

Here $\gamma = \sqrt{\kappa^2 - Z^2 \alpha^2}$, $I = \frac{(z_i + 1)^2}{\nu^2} Ry$ is the ionization energy with effective principal quantum number ν and $Ry = \frac{e^2}{2a_b}$.

The radial $p_{1/2}$ wave functions are written in terms of the radial s wave functions in the following way:

$$f_p = -\frac{A_p}{A_s} g_s, \quad (49)$$

$$g_p = i\frac{A_p}{A_s} f_s. \quad (50)$$

Here A_p is

$$A_p = \frac{Z\alpha}{(z_i + 1)^{1/2}} \frac{2\left(\frac{a}{2ZR}\right)^{1-\gamma}}{\Gamma(2\gamma + 1)} \left(\frac{Z}{a_b^3}\right)^{1/2} \times \left(\frac{I}{Ry}\right)^{3/4} \left(1 + \frac{9}{40}Z^2\alpha^2\right). \quad (51)$$

B. Relativistic wave function for a valence electron at $r \ll a_b/Z^{1/3}$

At short distances $r \ll a_b/Z^{1/3}$ the nuclear Coulomb potential is not screened and the valence electron energy may be neglected. The solution of the Dirac equation can be expressed in terms of Bessel functions - see e.g. [13].

$$f_\kappa = \frac{C}{r} \left[(\gamma + \kappa) J_{2\gamma}(y) - \frac{y}{2} J_{2\gamma-1}(y) \right] \quad (52)$$

$$g_\kappa = \frac{C}{r} (Z\alpha) J_{2\gamma}(y) \quad (53)$$

$$y = \sqrt{\frac{8Zr}{a_b}} \quad (54)$$

$$C = \frac{\kappa}{|\kappa|} \frac{1}{\sqrt{Za_b(z_i + 1)}} \left(\frac{I}{Ry}\right)^{3/4} \quad (55)$$

Again, we introduced factor $(z_i + 1)$ to account for ion wave functions.

C. Relativistic wave function for a valence electron at $r \ll a_b/Z$

The Bessel functions have power asymptotic at $r \ll a_b/Z$. From power expansions of (52) and (53) one obtains the following expression for the electron wave functions outside the nucleus [12, 13]:

$$f_\kappa(r) = \frac{1}{(z_i + 1)^{1/2}} \frac{\kappa}{|\kappa|} (\kappa - \gamma) \left(\frac{Z}{a_b^3}\right)^{1/2} \quad (56)$$

$$\times \left(\frac{I}{Ry}\right)^{3/4} \frac{2}{\Gamma(2\gamma + 1)} \left(\frac{a_b}{2Zr}\right)^{1-\gamma}$$

$$g_\kappa(r) = \frac{1}{(z_i + 1)^{1/2}} \frac{\kappa}{|\kappa|} Z\alpha \left(\frac{Z}{a_b^3}\right)^{1/2} \quad (57)$$

$$\times \left(\frac{I}{Ry}\right)^{3/4} \frac{2}{\Gamma(2\gamma + 1)} \left(\frac{a_b}{2Zr}\right)^{1-\gamma}$$

D. Ionisation potentials for isotope shift and King plot calculations

For all $s \rightarrow p$ transitions we approximate the ground s state ionisation potential to be 52200 cm^{-1} , as this is the average of the ionisation potentials for elements from Cf to No (which have Z from 98 to 102). Each of these elements have similar ionisation potentials that are readily accessible from the NIST database [31]. Ionisation potentials for s electrons were not readily available for elements Mt to Cn (Z from 109 to 112), therefore we assume that they also have a ground state I of 52200 cm^{-1} . The ionisation potential for the excited p state was estimated to be approximately 22300 cm^{-1} ; this was estimated by subtracting the $s \rightarrow p$ transition frequency in No which has been measured as 29961 cm^{-1} from the No ground state [32].

Furthermore, the p ground state ionisation energy in Lr is measured to be 40005 cm^{-1} [33]. The upper s state was found by subtracting the $p \rightarrow s$ calculated transition frequency of 20253 cm^{-1} [34] to give an ionisation potential of 19800 cm^{-1} . Recent atomic structure calculations were used to find the potentials for the ground p states and excited s states for Nh and Fl. For the Nh p state we used 59770 cm^{-1} and the s state ionisation potential of 23729 cm^{-1} [35]. Similarly, for the Fl p state we used 68868 cm^{-1} [36], a $p \rightarrow s$ transition energy of 43876 cm^{-1} [35] to give a s state ionisation potential of 24992 cm^{-1} .

Ionization potentials and transition energies for King plot non-linearity estimates were taken from the NIST database [31].

[1] Y. T. Oganessian, V. K. Utyonkov, Y. V. Lobanov, F. S. Abdullin, A. N. Polyakov, I. V. Shirokovsky, Y. S. Tsyganov, G. G. Gulbekian, S. L. Bogomolov, B. N. Gikal, et al., Nuclear Physics A **734**, 109 (2004),

ISSN 0375-9474, URL <http://www.sciencedirect.com/science/article/pii/S0375947404000259>.

[2] J. H. Hamilton, S. Hofmann, and Y. T. Oganessian, Annual Review of Nuclear and Particle Science

- 63**, 383 (2013), URL <http://dx.doi.org/10.1146/annurev-nucl-102912-144535>.
- [3] G. M. Fuller, A. Kusenko, and V. Takhistov, arXiv:1704.01129 [astro-ph, physics:hep-ph] (2017), arXiv: 1704.01129, URL <http://arxiv.org/abs/1704.01129>.
- [4] V. F. Gopka, A. V. Yushchenko, V. A. Yushchenko, I. V. Panov, and C. Kim, Kinematics and Physics of Celestial Bodies **24**, 89 (2008), ISSN 0884-5913, 1934-8401, URL <https://link.springer.com/article/10.3103/S0884591308020049>.
- [5] V. A. Dzuba, V. V. Flambaum, and J. K. Webb, Physical Review A **95**, 062515 (2017), URL <https://link.aps.org/doi/10.1103/PhysRevA.95.062515>.
- [6] E. Witten, Physical Review D **30**, 272 (1984), URL <https://link.aps.org/doi/10.1103/PhysRevD.30.272>.
- [7] J. C. Berengut, D. Budker, C. Delaunay, V. V. Flambaum, C. Frugiuele, E. Fuchs, C. Grojean, R. Harnik, R. Ozeri, G. Perez, et al., arXiv:1704.05068 [hep-ph, physics:physics, physics:quant-ph] (2017), arXiv: 1704.05068, URL <http://arxiv.org/abs/1704.05068>.
- [8] G. Racah, Nature **129**, 723 (1932), URL <http://www.nature.com/nature/journal/v129/n3263/abs/129723a0.html>.
- [9] J. E. Rosenthal and G. Breit, Physical Review **41**, 459 (1932), URL <https://link.aps.org/doi/10.1103/PhysRev.41.459>.
- [10] W. H. King, *Isotope Shifts in Atomic Spectra* (Springer Science & Business Media, 2013), ISBN 978-1-4899-1786-7, google-Books-ID: eEGCAAQBAJ.
- [11] V. M. Shabaev, Journal of Physics B: Atomic, Molecular and Optical Physics **26**, 1103 (1993), ISSN 0953-4075, URL <http://stacks.iop.org/0953-4075/26/i=6/a=011>.
- [12] I. I. Sobelman, *Introduction to the Theory of Atomic Spectra - 1st Edition* (Pergamon, 1972), URL <https://www.elsevier.com/books/introduction-to-the-theory-of-atomic-spectra/sobelman/978-0-08-016166-2>.
- [13] I. B. Khriplovich, *Parity nonconservation in atomic phenomena* (Gordon and Breach, 1991), 2nd ed., URL <https://www.osti.gov/scitech/biblio/6440853>.
- [14] F. Gebert, Y. Wan, F. Wolf, C. N. Angstmann, J. C. Berengut, and P. O. Schmidt, Physical Review Letters **115**, 053003 (2015), URL <https://link.aps.org/doi/10.1103/PhysRevLett.115.053003>.
- [15] G. Fricke and K. Heilig, *Nuclear Charge Radii*, no. 20 in Elementary Particles, Nuclei and Atoms (Springer-Verlag Berlin Heidelberg, 2004), ISBN 978-3-540-42829-9, URL <http://www.springer.com/gp/book/9783540428299>.
- [16] W. H. King, JOSA **53**, 638 (1963), URL <https://www.osapublishing.org/abstract.cfm?uri=josa-53-5-638>.
- [17] M. Puchalski and K. Pachucki, Hyperfine Interactions **196**, 35 (2010), ISSN 0304-3843, 1572-9540, URL <https://link.springer.com/article/10.1007/s10751-009-0137-z>.
- [18] A. B. Migdal, Journal of Experimental and Theoretical Physics **15**, 81 (1945).
- [19] J. S. Levinger, Physical Review **107**, 554 (1957), URL <https://link.aps.org/doi/10.1103/PhysRev.107.554>.
- [20] C. F. von Weizsäcker, Z. Phys. **96**, 431 (1935).
- [21] A. E. S. Green, Physical Review **95**, 1006 (1954), URL <https://link.aps.org/doi/10.1103/PhysRev.95.1006>.
- [22] L. D. D. Landau and E. M. Lifshitz, *Quantum mechanics : non-relativistic theory* (Pergamon, London, 1958).
- [23] J. Piekarewicz, B. K. Agrawal, G. Colò, W. Nazarewicz, N. Paar, P.-G. Reinhard, X. Roca-Maza, and D. Vretenar, Physical Review C **85**, 041302 (2012), URL <https://link.aps.org/doi/10.1103/PhysRevC.85.041302>.
- [24] J. A. R. Griffith, G. R. Isaak, R. New, and M. P. Ralls, Journal of Physics B: Atomic and Molecular Physics **14**, 2769 (1981), ISSN 0022-3700, URL <http://stacks.iop.org/0022-3700/14/i=16/a=007>.
- [25] C. W. P. Palmer and D. N. Stacey, Journal of Physics B: Atomic and Molecular Physics **15**, 997 (1982), ISSN 0022-3700, URL <http://stacks.iop.org/0022-3700/15/i=7/a=009>.
- [26] E. C. Seltzer, Physical Review **188**, 1916 (1969), URL <https://link.aps.org/doi/10.1103/PhysRev.188.1916>.
- [27] S. A. Blundell, P. E. G. Baird, C. W. P. Palmer, D. N. Stacey, and G. K. Woodgate, Journal of Physics B: Atomic and Molecular Physics **20**, 3663 (1987), ISSN 0022-3700, URL <http://stacks.iop.org/0022-3700/20/i=15/a=015>.
- [28] G. Torbohm, B. Fricke, and A. Rosén, Physical Review A **31**, 2038 (1985), URL <https://link.aps.org/doi/10.1103/PhysRevA.31.2038>.
- [29] C. Delaunay, R. Ozeri, G. Perez, and Y. Soreq, arXiv:1601.05087 [hep-ph, physics:physics, physics:quant-ph] (2016), arXiv: 1601.05087, URL <http://arxiv.org/abs/1601.05087>.
- [30] V. V. Flambaum and J. S. M. Ginges, Physical Review A **65**, 032113 (2002), URL <https://link.aps.org/doi/10.1103/PhysRevA.65.032113>.
- [31] A. Kramida, Y. Ralchenko, J. Reader, and NIST ASD Team, *NIST Atomic Spectra Database (ver. 5.3)* (National Institute of Standards and Technology, Gaithersburg, MD, 2017), URL <https://physics.nist.gov/asd>.
- [32] M. Laatiaoui, W. Lauth, H. Backe, M. Block, D. Ackermann, B. Cheal, P. Chhetri, C. E. Düllmann, P. van Duppen, J. Even, et al., Nature **538**, 495 (2016), ISSN 0028-0836, URL <http://www.nature.com/nature/journal/v538/n7626/abs/nature19345.html>.
- [33] T. K. Sato, M. Asai, A. Borschevsky, T. Stora, N. Sato, Y. Kaneya, K. Tsukada, C. E. Düllmann, K. Eberhardt, E. Eliav, et al., Nature **520**, 209 (2015), ISSN 0028-0836, URL <http://www.nature.com/nature/journal/v520/n7546/abs/nature14342.html>.
- [34] V. A. Dzuba, M. S. Safronova, and U. I. Safronova, Physical Review A **90**, 012504 (2014), URL <https://link.aps.org/doi/10.1103/PhysRevA.90.012504>.
- [35] T. H. Dinh and V. A. Dzuba, Physical Review A **94**, 052501 (2016), URL <https://link.aps.org/doi/10.1103/PhysRevA.94.052501>.
- [36] A. Landau, E. Eliav, Y. Ishikawa, and U. Kaldor, The Journal of Chemical Physics **114**, 2977 (2001), ISSN 0021-9606, URL <http://aip.scitation.org/doi/10.1063/1.1342763>.